



Intestinal phenotype is maintained by Atoh1 in the cancer region of intraductal papillary mucinous neoplasm

Nobuhiro Katsukura¹ | Sho Watanabe¹ | Tomoaki Shirasaki¹ | Shuji Hibiya¹ |
Yoshihito Kano^{2,3} | Keiichi Akahoshi⁴ | Minoru Tanabe⁴ | Susumu Kirimura⁵ |
Takumi Akashi⁵ | Masanobu Kitagawa⁶ | Ryuichi Okamoto^{1,7}  | Mamoru Watanabe^{1,8} |
Kiichiro Tsuchiya¹ 

¹Department of Gastroenterology and Hepatology, Graduate School, Tokyo Medical and Dental University, Tokyo, Japan

²Department of Clinical Oncology, Graduate School, Tokyo Medical and Dental University, Tokyo, Japan

³Department of Precision Cancer Medicine, Graduate School, Center for Innovative Cancer Treatment, Tokyo Medical and Dental University, Tokyo, Japan

⁴Department of Hepato-Biliary-Pancreatic Surgery, Graduate School, Tokyo Medical and Dental University, Tokyo, Japan

⁵Department of Surgical Pathology, Graduate School, Tokyo Medical and Dental University, Tokyo, Japan

⁶Department of Comprehensive Pathology, Graduate School, Tokyo Medical and Dental University, Tokyo, Japan

⁷Center for Stem Cell and Regenerative Medicine, Graduate School, Tokyo Medical and Dental University, Tokyo, Japan

⁸Advanced Research Institute, Graduate School, Tokyo Medical and Dental University, Tokyo, Japan

Correspondence

Kiichiro Tsuchiya, Department of Gastroenterology and Hepatology, Graduate School, Tokyo Medical and Dental University, 1-5-45 Yushima, Bunkyo-ku, Tokyo 113-8519, Japan.
Email: kii.gast@tmd.ac.jp

Funding information

The Practical Research for Innovative Cancer Control, Rare/Intractable Diseases from Japan Agency for Medical Research and Development (AMED), Grant/Award Number: 15Ack0106017h0002 and 16ck0106017h0003; Research Grant of the Princess Takamatsu Cancer Research Fund; scientific Research, from the Japanese Ministry of Education, Culture, Sports, Science and Technology, Grant/Award Number: 17H06654, 17K15930, 17K159301, 17K19513 and 18H02791; Japan Foundation for Applied Enzymology; the Health and Labor Sciences Research Grant from the Japanese Ministry of Health, Labor and Welfare (MHLW), Grant/Award

Abstract

Intraductal papillary mucinous neoplasm (IPMN) is a precancerous lesion of pancreatic cancer. Although there are 4 types of IPMN, among which intestinal-type IPMN is likely to progress into invasive cancer known as colloid carcinoma, no information regarding the involvement of the intestinal phenotype in the carcinogenesis of IPMN exists. The present study was conducted to explore how the intestinal differentiation system is maintained during the tumor progression of intestinal-type IPMN using surgical resection specimens. Results showed that Atoh1, a critical transcriptional factor for intestinal differentiation toward the secretory lineages of intestinal epithelial cells, was expressed in an invasive-grade IPMN. To determine the function of Atoh1 in pancreatic cancer, we generated a pancreatic ductal adenocarcinoma (PDAC) cell line overexpressing Atoh1. In a xenograft model, we successfully induced an IPMN phenotype in PDAC cells via Atoh1 induction. Finally, for the first time, we discovered that GPA33 is expressed in intestinal-type IPMN, thereby suggesting a novel target for cancer therapy. In conclusion, the intestinal differentiation system might be maintained during tumor progression of intestinal-type IPMN. Further analysis of the

Abbreviations: 5-FU, 5-fluorouracil; AGR2, anterior gradient 2; Atoh1, atonal bHLH transcription factor 1; CA2, carbonic anhydrase 2; CDX2, caudal type homeobox 2; ELDA, extreme limiting dilution analysis; FXRD3, FXRD domain containing ion transport regulator 3; GNAS, Guanine nucleotide-binding protein G(s) subunit alpha isoforms short; GPA33, glycoprotein A33; HD-6, human defensin alpha 6; Hes1, hes family bHLH transcription factor 1; IPMN, intraductal papillary mucinous neoplasm; MUC13, mucin 13; MUC2, mucin 2; Ngn3, neurogenin 3; PDAC, pancreatic ductal adenocarcinoma; PDX1, pancreatic and duodenal homeobox 1; REG4, regenerating family member 4; RIT, radioimmunotherapy; RNF43, ring finger protein 43; SMAD4, Mothers against decapentaplegic homolog 4; SOX9, SRY-box transcription factor 9; TFF3, trefoil factor 3; TP53, tumor protein p53.

This is an open access article under the terms of the Creative Commons Attribution-NonCommercial License, which permits use, distribution and reproduction in any medium, provided the original work is properly cited and is not used for commercial purposes.

© 2020 The Authors. *Cancer Science* published by John Wiley & Sons Australia, Ltd on behalf of Japanese Cancer Association.

Number: 14526073

function of Atoh1 in IPMN might be useful for understanding the molecular mechanism underlying the malignant potential during the tumor progression of IPMN.

KEYWORDS

Atoh1, differentiation, GPA33, intestinal type, intraductal papillary mucinous neoplasm

1 | INTRODUCTION

IPMN of the pancreas is a mucin-producing epithelial tumor in which the major outcome is tumor progression from dysplasia to invasive cancer.¹ Clinically, main duct (MD) and mixed-type (MT) IPMNs involving the major pancreatic duct itself have a risk for malignancy, whereas IPMN cysts confined to secondary branches (branch duct type, BD) are associated with a much lower rate of malignancy. Gene mutations in IPMN have been focused as a molecular mechanism underlying the tumor progression in IPMN. Mutations in guanine nucleotide-binding protein G(s) subunit alpha isoforms short (GNAS) possibly play a pivotal role in the development of IPMNs,^{2,3} a concept that has been confirmed by numerous molecular studies of human tissues and genetically engineered mouse models. Although gene mutations for ring finger protein 43 (RNF43), Mothers against decapentaplegic homolog 4 (SMAD4), and tumor protein p53 (TP53) have been reported as the sequential progression of IPMN into invasive cancer,⁴ further elucidation of the mechanisms underlying IPMN progression into invasive cancer may be necessary. A recently conducted detailed molecular analysis of precisely evaluated microdissected tissues from human clinical samples of IPMNs, including invasive cancer, disclosed the following distinct pathways responsible for tumor progression from IPMN into invasive cancer: sequential, de novo, and branch-off.⁵ However, the molecular mechanism underlying the acquisition of malignant potential during tumor progression in IPMN has not been elucidated. From another viewpoint, IPMN includes several distinct histopathological subtypes such as gastric, intestinal, pancreatobiliary, and oncocytic.⁶ Intestinal-type IPMN is characterized by intestinal-type papillae comprising tall columnar cells with cigar-shaped nuclei and abundant cytoplasm that is stained with Alcian blue. Intestinal-type IPMN frequently exhibits tumor progression from dysplasia to invasive cancer termed as colloid carcinoma.⁷ The initial belief was that GNAS mutation is associated with intestinal-type IPMN or mucinous (colloid-type) carcinoma.⁸ However, the evidence obtained using human specimens, as well as genetically engineered mouse models, did not indicate that GNAS directly regulates such phenotypes. Therefore, determining the mechanism by which the intestinal phenotype of IPMN regulates the tumor progression of IPMN independent of gene mutation is important to understand the carcinogenesis of intestinal-type IPMN. Both caudal type homeobox 2 (CDX2) and mucin 2 (MUC2), which are intestinal-specific genes, are expressed in IPMN.⁹ The expression of CDX2 in gastric-type IPMN suggests that CDX2 precedes the expression of MUC2 and maturation of intestinal features.¹⁰ However, no information regarding the precise role of CDX2 expression during

the tumor progression of intestinal-type IPMN has been reported. Furthermore, whether the systemic mechanism underlying the intestinal differentiation is reflected in intestinal-type IPMN remains unknown. Atonal bHLH transcription factor 1 (Atoh1), which is an essential gene for the differentiation toward goblet cells,^{11,12} plays numerous roles in the malignant potential of a variety of tumors based on intestinal metaplasia such as intestinal-type gastric cancer and esophageal cancer with Barrett's esophagus.¹³ However, there have been no reports on the expression and role of Atoh1 in the intestinal-type IPMN. Therefore, we conducted the present study to elucidate the effect of "intestinal-type" mediated by Atoh1 on the tumor progression of IPMN.

In the present study, Atoh1 was expressed in each grade of intestinal-type IPMN. Overexpression of Atoh1 in the pancreatic ductal adenocarcinoma (PDAC) cell line induced the expression of intestinal phenotypic genes, which reflects the expression in a high-grade/invasive region of intestinal-type IPMN. Finally, we detected that glycoprotein A33 (GPA33), which is a promising target for colon cancer therapy, was expressed in the cancer region of the intestinal-type IPMN.

2 | MATERIALS AND METHODS

2.1 | Human samples

Human tissue specimens were obtained from patients who underwent surgical resection for PDAC or IPMN at Tokyo Medical and Dental University Hospital between 2011 and 2020. Details of the patients are listed in Tables 1 and S1. The grade of intestinal-type IPMN was classified using the 2019 WHO classification of tumors of the digestive system.¹⁴ TNM classification of PDAC are summarized based on the 8th edition of the UICC TNM classification. The present study was approved by the Ethics Committee on Human Subjects of Tokyo Medical and Dental University Hospital.

2.2 | Histology and immunofluorescence

Histological analysis of human and xenograft samples was conducted using hematoxylin and eosin-stained sections or Alcian blue-stained sections prepared from paraffin sections. Immunofluorescence analyses were conducted using paraffin-embedded sections. Tissue sections were stained after microwave treatment (200 W, 10 min) in 10 mmol/L citrate buffer. For cell analysis, cells were fixed as

TABLE 1 Patient information

Intestinal-type IPMN patient information									
Patients	Age	Gender	Size	Location	Differentiation	Type	Low	High	Invasive
(A)									
1	55	F	20	Head	Low	Mixed	+	NA	NA
2	58	F	76	Tail	Low	BD	+	NA	NA
3	79	F	120	Body	Low	MD	+	NA	NA
4	63	M	18	Head	Low	BD	+	NA	NA
5	75	M	25	Head	Low	Mixed	+	NA	NA
6	64	M	32	Head	High	Mixed	+	+	NA
7	67	M	75	Head	High	Mixed	+	+	NA
8	76	M	50	Head	High	Mixed	+	+	NA
9	61	M	160	All	Invasive	Mixed	+	+	+
10	66	F	25	Head	Invasive	MD	NA	+	+
11	79	F	110	Head	Invasive	Mixed	+	+	+
12	80	M	65	Head	Invasive	Mixed	+	+	+
13	72	M	43	Head	Invasive	Mixed	+	+	+
PDAC patient information									
Patients	Age	Gender	Size	Location	T stage	N stage	M stage	TNM stage	Differentiation
(B)									
14	77	M	27	Head	T3	N0	M0	stageIII	por
15	53	F	19	Body	T1	N0	M0	stageI	tub2
16	80	F	45	Head	T4	N1	M0	stageIVa	tub2
17	69	M	30	Body	T3	N0	M0	stageIII	tub1
18	72	F	25	Head	T4	N1	M0	stageIVa	tub2
19	66	M	32	Head	T3	N1	M0	stageIII	tub2
20	68	M	40	Head	T4	N1	M0	stageIVa	tub2
21	48	F	50	Body	T3	N0	M0	stageIII	tub2
22	68	M	40	Head	T3	N1	M0	stageIII	tub2
23	66	M	70	Body	T4	N1	M0	stageIVa	tub2

Size: Tumor size (mm); BD: branched type; MD: main duct type; NA: not applicable.

The grade of intestinal-type IPMN was classified using the 2019 WHO classification of tumors of the digestive system. TNM classifications are summarized based on the 8th edition of the UICC TNM classification.

described previously.¹⁵ An Atoh1 antibody, originally generated by immunizing rabbits with Atoh1 peptide, was used as described previously.¹⁶ Anti-CDX2 (#3977; Cell Signaling Technology, Danvers, MA, USA), anti-MUC2 (Ccp58) (sc-7314; Santa Cruz Biotechnology, Texas, USA), anti-human defensin alpha 6 (HD-6) (HPA019462; Atlas Antibodies, Bromma, Sweden), and anti-GPA33 (HPA018858; Atlas Antibodies) were also used. Primary antibodies were visualized using secondary antibodies conjugated to either Alexa-594 or Alexa-488 (Invitrogen, Carlsbad, CA, USA). Sections were mounted using VectaShield mounting medium containing DAPI (Vector Laboratories, Burlingame, CA) and visualized under a confocal laser fluorescence microscope (BZ-X700; Keyence, Tokyo, Japan) or confocal fluorescence microscope (FLUOVIEW FV10i, OLYMPUS, Tokyo, Japan). To quantify the immunofluorescence images, a BZX analyzer (Keyence) was used. Briefly, the cell nuclei in the epithelial

layer were detected by DAPI staining. Fluorescence intensity of CDX2 and Atoh1 in nuclei in more than 100 cells per field in each grade of IPMN was measured automatically. The fluorescence intensity of GPA33 in the cytoplasm in 10 cells in each grade of IPMN was measured. The average fluorescence intensity in those cells is shown as the expression in each grade of IPMN.

2.3 | Xenograft transplantation

Panc1 cells expressing mCherry or CDX2 or mCherry-Atoh1 were injected into 6-wk-old BALB/cAJcl-nu/nu mice (Clea Japan, Inc) using a fine needle after placing the mouse under general anesthesia. Tumor volumes transplanted with 5 000 000 cells were recorded weekly. Tumor formation was evaluated after an 8-wk period after

inoculation. Mice were sacrificed by cervical dislocation and tumors were collected immediately for histological examination and PCR. For PCR assay, the tumors were treated with RNAlater (Qiagen). All experimental protocols involving animals were approved by the Animal Experimentation Ethics Committee of Tokyo Medical and Dental University (Tokyo Japan). The other material and methods are described in Doc S1.

3 | RESULTS

3.1 | Atoh1 is highly expressed in the high-grade dysplasia of intestinal-type IPMN

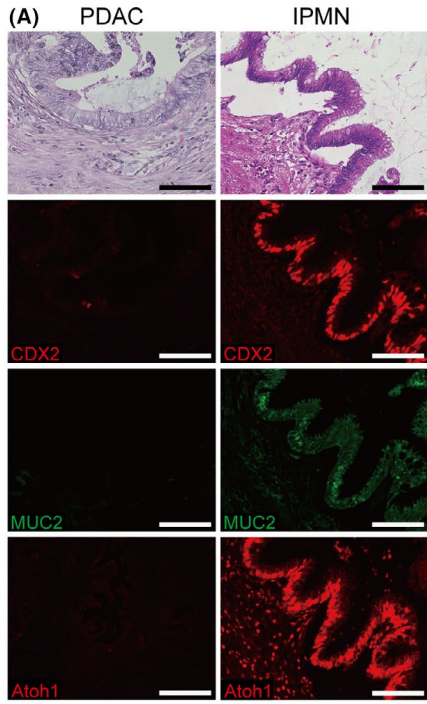
First, the expression of intestinal phenotypic genes in intestinal-type low-grade IPMN was evaluated by immunofluorescence. As reported earlier, both CDX2 and MUC2 were expressed in intestinal-type IPMN, whereas both proteins were not expressed in PDAC (Figure 1A). To confirm whether the intestinal differentiation sequence of intestinal epithelial cells was preserved in intestinal-type IPMN, Atoh1 expression, a critical transcription factor for the differentiation toward secretory lineage, was evaluated. As anticipated, Atoh1 was expressed in intestinal-type IPMN but not in PDAC (Figures 1A and S1). Atoh1 expression was also detected in various grades of 13 patients with intestinal-type IPMN as well as in CDX2 and MUC2. By contrast, no Atoh1 expression was detected in the region of PDAC, except for 1 patient (Figure 1B). Moreover, Atoh1 was not detected in the other type of IPMN (Figure S1). The expression levels of both CDX2 and Atoh1 remained unchanged among patients with each grade of intestinal-type IPMN (Figure 1C). To evaluate thoroughly the effect of intestinal phenotype on carcinoma sequence in IPMN, we analyzed the expression of CDX2 and Atoh1 in each grade of an identical individual with intestinal-type IPMN. A representative section of the operative tissue showed various grades of IPMN from low-grade to invasive carcinoma in a section (Figure 1D). The expression of both CDX2 and Atoh1 was gradually increased from low-grade to invasive carcinoma (Figure 1E). The expression levels of both CDX2 and Atoh1 in the high-grade region of

IPMN was significantly higher compared with that in the low-grade region of IPMN among 6 patients with IPMN who had both low- and high-grade IPMN in the same section (Figure 1F). The expression levels of both CDX2 and Atoh1 in the invasive region of IPMN was equal to that in high-grade IPMN in 5 patients with IPMN who had both high-grade dysplasia and invasive region in the same section (Figure 1G).

3.2 | Atoh1 induces intestinal phenotype in a PDAC cell line

Both CDX2 and Atoh1 exhibited high expression in the cancer region of IPMN, suggesting that the malignant phenotype of intestinal-type IPMN is affected by these proteins. Either CDX2 or Atoh1 was transfected into the PDAC cell line Panc1. RT-PCR and immunofluorescence were used to confirm transfection of CDX2 and Atoh1 (Figure 2A,B). In the cascade of the intestinal differentiation system, CDX2 is located upstream of Atoh1 and directly upregulates Atoh1 expression by binding to the Atoh1 enhancer element.¹⁷ However, CDX2 did not induce Atoh1 expression in Panc1 cells. By contrast, Atoh1 induced expression of CDX2 (Figure 2B). We also evaluated a series of intestinal phenotypic genes and found that MUC2 and trefoil factor 3 (TFF3), both of which are phenotypic genes for goblet cells, were slightly induced by Atoh1, but not by CDX2. HD-6 and neurogenin 3 (Ngn3), which are phenotypic genes for Paneth cells and endocrine cells, respectively, were not significantly induced by Atoh1 and CDX2. Carbonic anhydrase 2 (CA2), which is a phenotypic gene for absorptive cells, was significantly induced by CDX2 and Atoh1. Hes family bHLH transcription factor 1 (Hes1), which is affected by the Notch signal, was not influenced by CDX2 and Atoh1. The pancreatic cell markers, pancreatic and duodenal homeobox 1 (PDX1) and SRY-box transcription factor 9 (SOX9), were reciprocally induced by Atoh1 (Figure 2C). Reportedly, PDX1 is highly expressed in IPMN, whereas the SOX9-positive rate gradually decreases during tumor progression,¹⁸ suggesting that Atoh1 expression in PDAC cell line reflects the tumor progression in IPMN.

FIGURE 1 Intestinal phenotypic genes were expressed in each grade of intestinal-type IPMN but not in PDAC. A, HE and immunofluorescence staining of intestinal-type IPMN and PDAC specimens revealed the expression of intestinal phenotypic genes (CDX2, MUC2, and Atoh1) in intestinal-type IPMN but not in PDAC. The image of PDAC is from patient no. 17. The image of IPMN is low-grade dysplasia of patient no. 10. Scale bar, 100 μ m. B, Evaluation of intestinal phenotypic genes in 13 patients with intestinal-type IPMN and 10 patients with PDAC by immunofluorescence staining. Each cell shows the qualitative results of the genes (from left, CDX2, MUC2, Atoh1) in each grade of each patient. The positive rate is listed at the bottom of the table. NA, not applicable. C, The immunofluorescence staining in Figure 1B was quantitatively evaluated. Fluorescence intensity in more than 100 cells of each grade of each patient were quantified using the BZX analyzer (Keyence), and its average was shown in dots. Bars represent means (\pm SEM). D, A representative image of the location of each grade in a section generated from operative tissue of intestinal-type IPMN (patient no. 12). Various grades of IPMN were located in a section. The area of each grade represented in each color line was decided by a pathologist. E, HE and immunofluorescence staining of CDX2 and Atoh1 in a section of an identical patient (no. 12). Scale bars, 100 μ m. F, The expression levels of both CDX2 and Atoh1 in the same section with low-grade and high-grade intestinal-type IPMN. Quantified as in Figure 1C. The dots of the same patient were connected by a line. An identical comparison between low-grade and high-grade IPMN in 6 patients. G, The expression levels of both CDX2 and Atoh1 in the same section with high-grade and invasive regions of intestinal-type IPMN. An identical comparison between high-grade and invasive region of 5 patients. * $P < .05$. NS, not significant



(B) IPMN

Patients	CDX2/MUC2/Atoh1		
	Low	High	Invasive
1	+/-/+	N.A.	N.A.
2	+/+/+	N.A.	N.A.
3	+/-/+	N.A.	N.A.
4	+/+/+	N.A.	N.A.
5	+/+/+	N.A.	N.A.
6	+/+/+	+/+/+	N.A.
7	-/+/+	+/+/+	N.A.
8	+/+/+	+/+/+	N.A.
9	+/+/+	+/+/+	+/+/+
10	N.A.	+/-/+	+/-/+
11	+/+/+	+/+/+	+/+/+
12	+/+/+	+/+/+	+/-/+
13	N.A.	+/+/+	+/+/+
Total			
CDX2	10/11	8/8	5/5
MUC2	9/11	7/8	3/5
Atoh1	11/11	8/8	5/5

PDAC

Patients	CDX2/MUC2/Atoh1
14	-/-/-
15	-/-/-
16	-/-/-
17	-/-/-
18	-/-/-
19	-/-/-
20	-/-/-
21	-/-/-
22	-/-/-
23	-/-/+
Total	
CDX2	0/10
MUC2	0/10
Atoh1	1/10

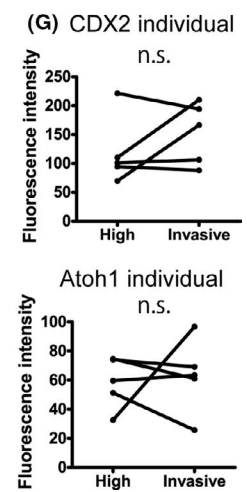
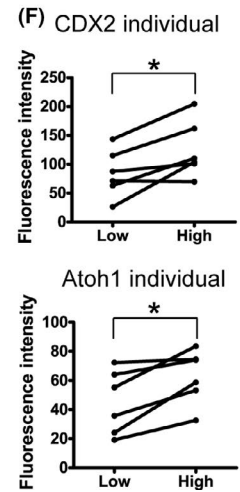
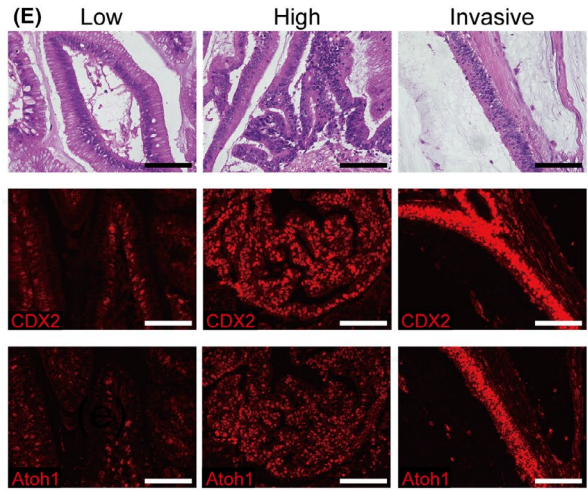
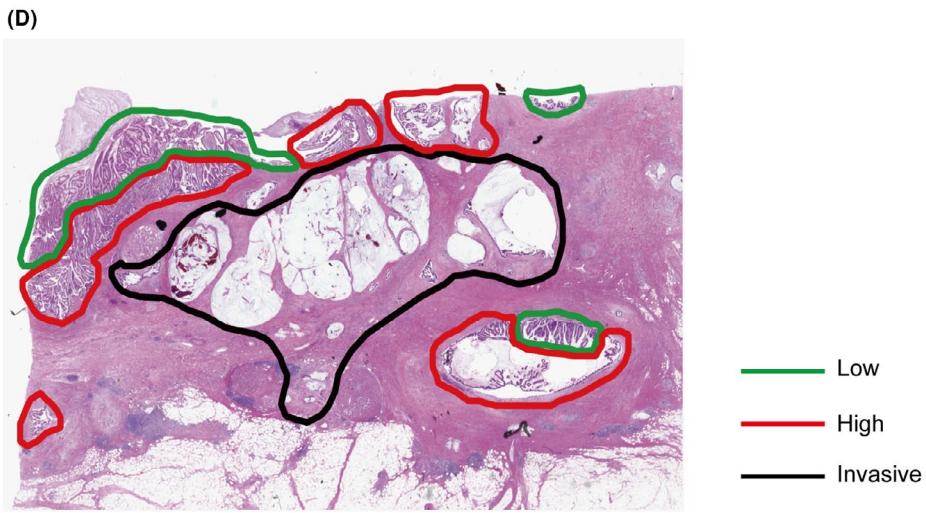
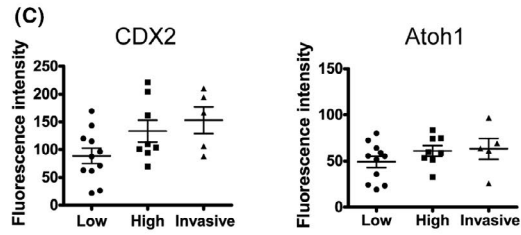
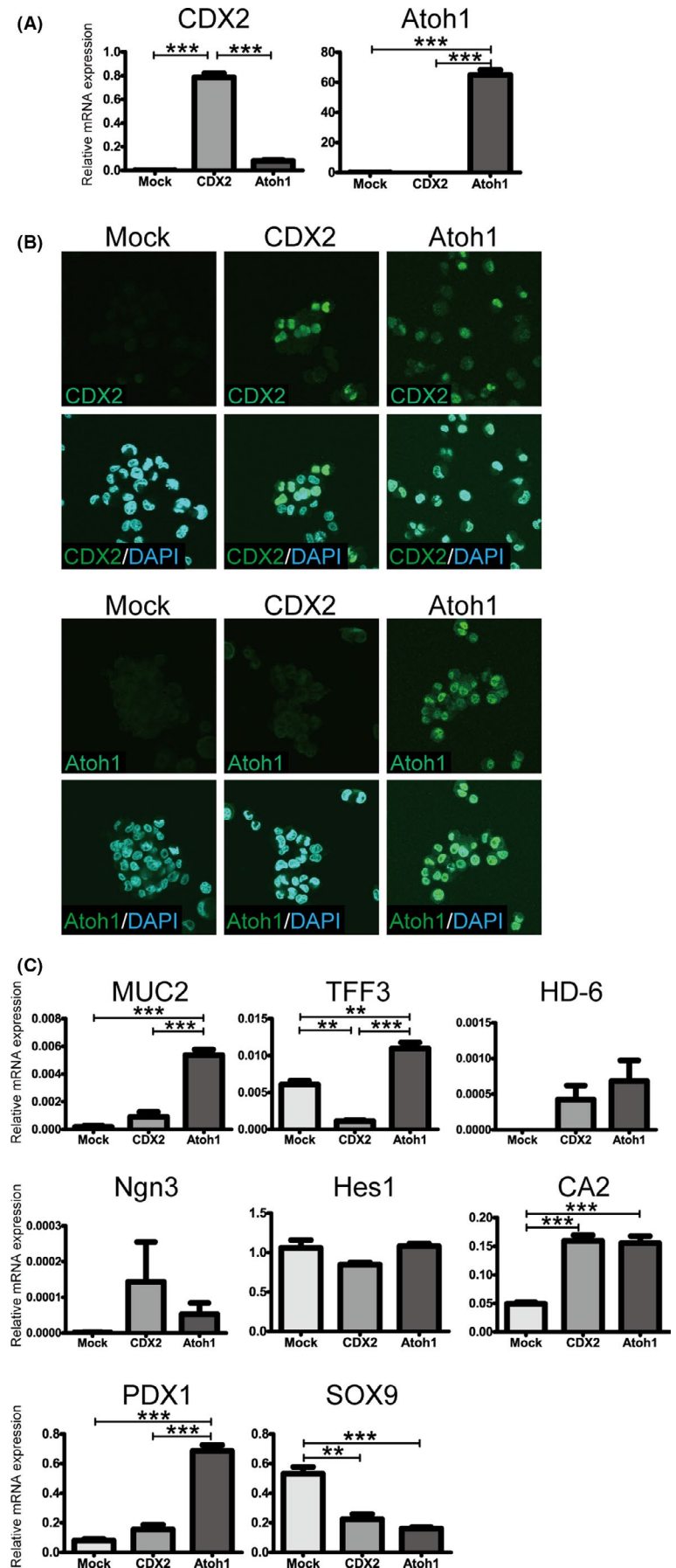


FIGURE 2 Atoh1 induces intestinal phenotype in the PDAC cell line. A, RT-PCR analysis of CDX2 (left panel) and Atoh1 (right panel) in transfected Panc1 cells. CDX2 was expressed in not only CDX2 transfected cells, but also Atoh1 transfected cells. Atoh1 was expressed only in Atoh1 transfected cells. Mock, mCherry expressing cells. $***P < .001$, $n = 3$. NS, not significant. B, Immunofluorescence of CDX2 (upper figures) and Atoh1 (lower figures) in transfected Panc1 cells. C, RT-PCR analysis of goblet cell marker genes (MUC2 and TFF3), Paneth cell marker gene (*HD-6*), endocrine cell marker gene (*Ngn3*), absorptive cell marker genes (*HES1* and *CA2*), and pancreatic cell marker genes (*PDX1* and *SOX9*). The degree of mRNA expression was normalized to that of β -actin. LS174T (the mucinous phenotype of a colon cancer cell line) was used as a standard for quantitative mRNA expression analysis. $**P < .01$, $***P < .001$, $n = 3$. NS, not significant



3.3 | Atoh1 might suppress invasiveness in the malignant potential of Panc1 cells

We next evaluated the effect of CDX2 and Atoh1 on various malignant potentials of Panc1 cells. We first explored the effect of CDX2 and Atoh1 on invasiveness, a type of malignant potential, in Panc1 cells. Both CDX2-expressing and Atoh1-expressing cells exhibited

reduced migration (Figure 3A,B). Proliferation assay demonstrated a slight reduction of proliferation in CDX2-expressing cells (Figure 3C). Then, we evaluated the chemoresistance of CDX2-expressing and Atoh1-expressing cells and observed that 5-FU-induced apoptosis was suppressed in Atoh1-expressing cells, resulting in high viability (Figure 3D). In the spheroid-forming assay, both CDX2-expressing and Atoh1-expressing cells yielded smaller numbers of spheroids

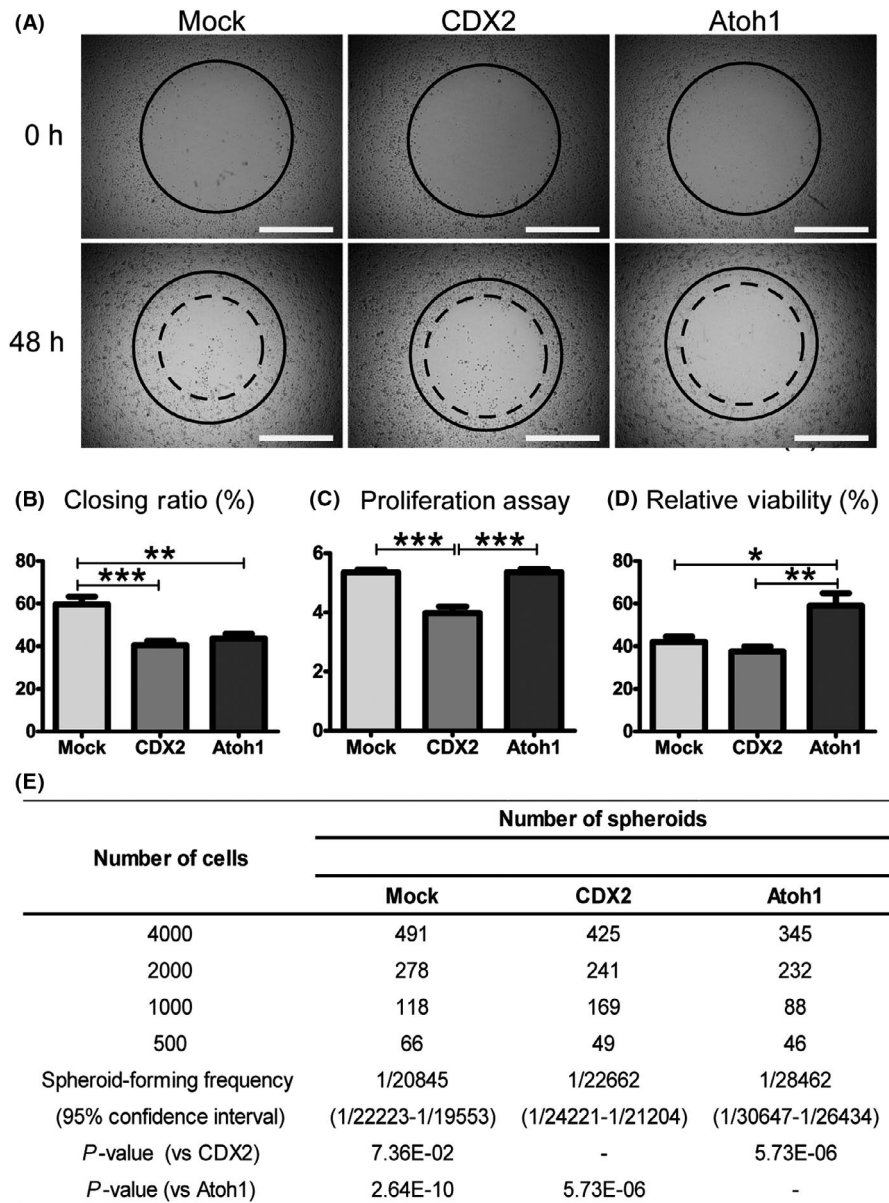


FIGURE 3 Atoh1 might suppress invasiveness in the malignant potential of Panc1 cells. A, Migration assay revealed reduced migration in both CDX2-expressing and Atoh1-expressing cells. The images show the cells after seeding. The cell-free zone was indicated by a solid line at 0 h and a broken line at 48 h after seeding. Scale bar, 1000 μ m. B, The ratio of the remaining vacant areas is shown. The vacant areas of both CDX2-expressing and Atoh1-expressing cells were smaller than that of Mock cells at 48 h after the cells were seeded. ** $P < .01$, *** $P < .001$, $n = 6$. C, The MTS assay revealed a slightly decreased proliferation rate in CDX2-expressing cells. The cell proliferation ratio was calculated by dividing the titer of cells cultured for 72 h by that of cells cultured for 24 h. *** $P < .001$, $n = 6$. D, Cells were treated with 5-fluorouracil (5-FU; 50 μ M) or DMSO for 48 h to examine chemoresistance. Relative viability (%) was calculated by dividing the cell proliferation ratio of the 5-FU treated group by that of the untreated group. The MTS assay showed that 5-FU-induced apoptosis was suppressed in Atoh1-expressing cells. * $P < .05$, ** $P < .01$, $n = 6$. E, Cells at various concentrations (4000, 2000, 1000, and 500 cells/well) were cultured. After 14 d, the number of spheroids was counted. The 95% confidence interval for spheroid-forming frequency was calculated using a software application for limiting dilution analysis, ELDA. $n = 6$

generated from single cells than Mock. The results of ELDA indicated a slight decrease in the number of cancer stem cells in both CDX2-expressing and Atoh1-expressing cells (Figure 3E). Overall, the in vitro results obtained using CDX2-expressing and Atoh1-expressing cells suggested that Atoh1 induces the goblet cell phenotype rather than CDX2 in Panc1 cells. Both Atoh1 and CDX2 did not exert a clear effect on the malignant potential of Panc1, although the invasiveness was suppressed by both CDX2 and Atoh1. The overexpression of neither CDX2 nor Atoh1 could induce the intestinal phenotype in other cell lines derived from PDAC, such as MIA-Paca2 and SW1990.

3.4 | Atoh1 acquires the mucinous phenotype of pancreatic cancer cells in vivo

To further determine the effect of CDX2 and Atoh1 on the malignant phenotype of IPMN in vivo, CDX2- and Atoh1-expressing Panc1 cells were inoculated into nude mice. Surprisingly, larger tumors were generated from Atoh1-expressing cells compared with from CDX2-expressing Panc1 cells (Figure 4A). The results of ELDA also revealed a significant tumorigenicity of Atoh1-expressing cells, but not CDX2-expressing cells (Figure 4B). The pathological findings of each tumor indicated the generation of signet cell carcinoma with mucinous formation in Atoh1-expressing tumors, whereas no alternative findings were detected in CDX2-expressing tumors compared with those in Mock tumors (Figure 4C,D). We also validated the expression of transfected genes in tumors. Although CDX2 was expressed in tumors inoculated with CDX2-expressing cells, Atoh1 protein was not induced in CDX2-expressing tumors, resulting in a MUC2-negative tumor. By contrast, not only Atoh1, but also CDX2, was expressed in tumors inoculated with Atoh1-expressing cells, resulting in MUC2-positive tumors. We had earlier reported that HD-6 was directly induced by Atoh1, which binds to the promoter region of HD-6.¹⁹ As expected, HD-6 was expressed in Atoh1-expressing tumors but not in CDX2-expressing tumors (Figure 4E). We then evaluated the intestinal phenotypes of tumors via RT-PCR and found that MUC2, TFF3, and HD-6 were markedly induced in Atoh1-expressing tumors compared with those in Atoh1-expressing cells in in vitro culture. Ngn3 was also induced in both CDX2-expressing and Atoh1-expressing tumors compared with each cell in in vitro culture, respectively. PDX1 was also induced in Atoh1-expressing tumors, suggesting that Atoh1 acquires the intestinal phenotype of IPMN during tumor progression. To confirm whether

Atoh1-expressing tumors reflect the phenotype of the intestinal-type IPMN, we evaluated the expression of HD-6 in IPMN. HD-6 expression was found in some patients with IPMN but not in those with PDAC, except for 1 patient in whom Atoh1 was expressed in PDAC (Figure S2).

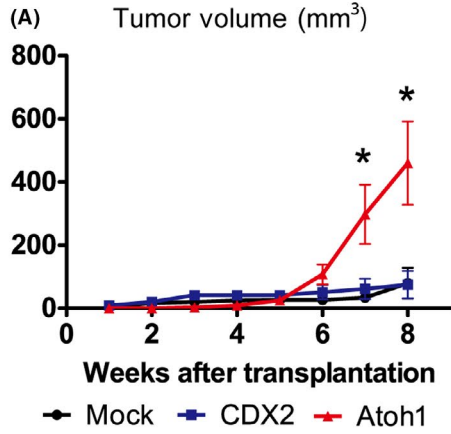
3.5 | Atoh1 enhances the expression of GPA33 in IPMN

Because Atoh1-expressing tumors in Panc1 cells, but not CDX2-expressing tumors, might mimic the process of tumor progression of IPMN, we conducted a microarray analysis to evaluate the comprehensive gene expression of Atoh1-expressing tumors. Several genes that were markedly upregulated in Atoh1-expressing tumors were extracted (Tables 2 and S3). Genes that were associated with the malignant potential of IPMN, such as regenerating family member 4 (REG4),²⁰ mucin 13 (MUC13),²¹ anterior gradient 2 (AGR2),²¹ and FXYD domain containing ion transport regulator 3 (FXYD3),²¹ were involved in upregulation by Atoh1, suggesting that Atoh1-expressing tumors reflected the malignant phenotype of IPMN. Finally, we focused on the expression of a representative gene for the intestinal phenotype in IPMN. Several intestinal phenotypic genes were highly induced in Atoh1-expressing tumors (Tables 2 and S3). GPA33 is one of the most broadly expressed genes in the intestine.²² It is also a biomarker for not only colon cancer²³ but also gastric cancer²⁴ and Barrett's esophageal cancer,²⁵ both of which are based on intestinal metaplasia. We confirmed the induction of GPA33 in Atoh1-expressing tumors, but not CDX2-expressing tumors (Figure 5A,B). Moreover, we detected the expression of GPA33 in intestinal-type IPMN but not the other type of IPMN (Figure S1). Furthermore, we detected a significantly higher expression level of GPA33 in high-grade rather than in low-grade IPMN in 6 patients with IPMN who had both low-grade and high-grade dysplasia in the same section (Figure 5C,D). The expression levels of GPA33 in the invasive region of IPMN was equal to that in high-grade IPMN in 5 patients with IPMN who had both high-grade and invasive regions in the same section (Figure 5E,F).

4 | DISCUSSION

The present study demonstrated that not only CDX2 but also Atoh1 was expressed in various grades of intestinal-type IPMN. Especially,

FIGURE 4 Atoh1 acquires the mucinous phenotype of pancreatic cancer cells in vivo. A, Growth curves of pancreatic carcinoma xenografts in nude mice are shown. Data are presented as mean \pm standard deviation. Larger tumors were generated from Atoh1-expressing cells than others. *Significant difference between Atoh1 and the other 2 groups is indicated. $P < .01$, $n = 4$. B, Atoh1-expressing cells exhibited significant tumorigenicity. Cells at various concentrations were inoculated into mice ($n = 4$ per each group). After 8 wk, the tumor-initiating frequency was calculated. The tumor-forming frequency (the average number of cells determined to be required to cause tumor growth) and the 95% confidence interval were calculated using a software application for limiting dilution analysis, ELDA. C, HE staining in xenograft demonstrated the generation of signet cell carcinoma in only Atoh1-expressing tumors. D, Alcian blue staining in xenograft demonstrated mucinous formation in only Atoh1-expressing tumors. C, D, The upper figure shows the low magnification image (scale bars, 100 μ m), and the lower figure shows the high magnification image (scale bars, 10 μ m). E, Immunofluorescence staining of CDX2, Atoh1, MUC2, and HD-6 in xenograft revealed that Atoh1-expressing tumors expressed not only Atoh1 but also CDX2; they also expressed MUC2 and HD-6. Scale bars, 100 μ m. F, RT-PCR analysis of xenograft revealed that Atoh1-expressing tumors reflect the phenotype of the intestinal-type IPMN. * $P < .05$, ** $P < .01$, *** $P < .001$, $n = 3$. NS, not significant



(B)

Number of cells	Developing tumor		
	Mock	CDX2	Atoh1
5000000	4/4	4/4	4/4
1000000	2/4	3/4	4/4
500000	2/4	2/4	4/4
50000	1/4	0/4	4/4
Tumor-forming frequency	1/874954	1/759573	1/1
(95% confidence interval)	(1/2141413-1/357495)	(1/1842050-1/313211)	(1/77909-1/1)
<i>P</i> -value (vs CDX2)	0.824		2.63E-06
<i>P</i> -value (vs Atoh1)	8.40E-07	2.63E-06	

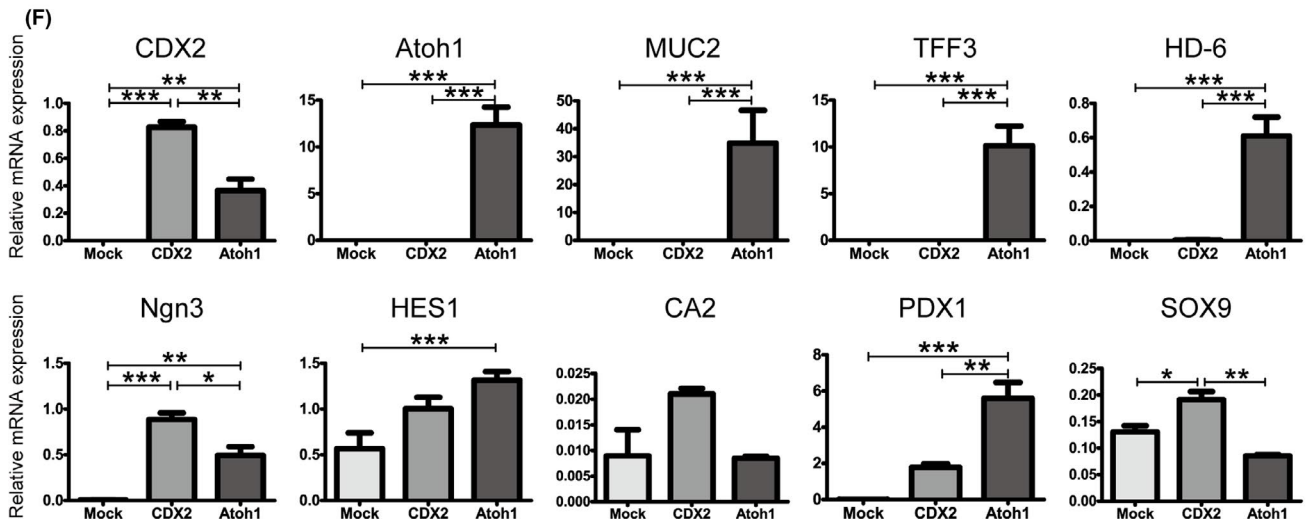
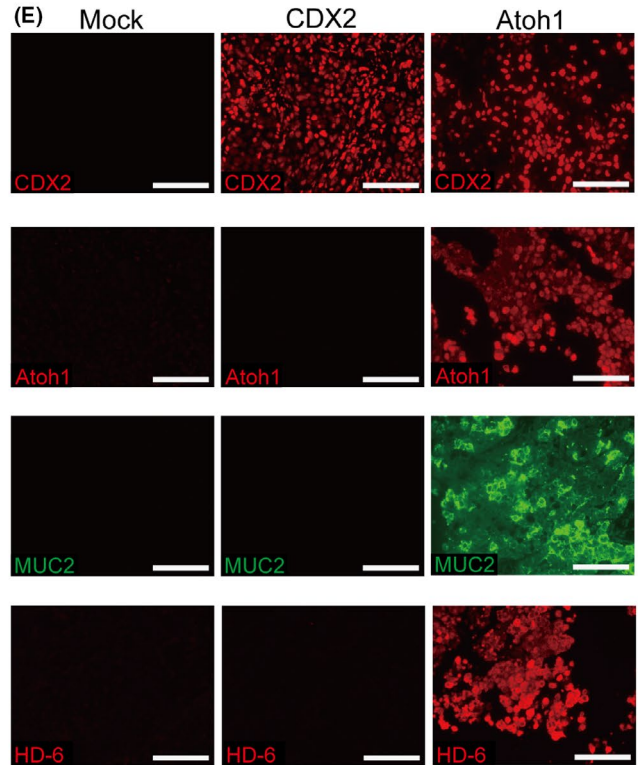
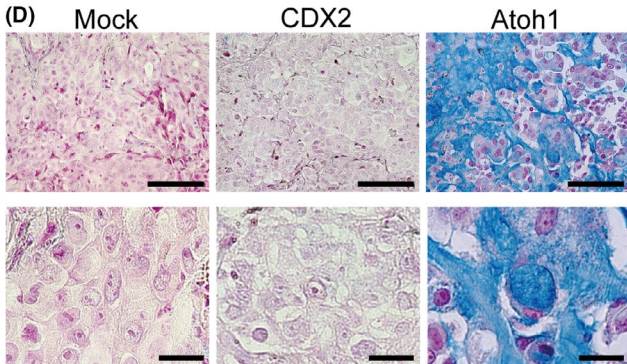
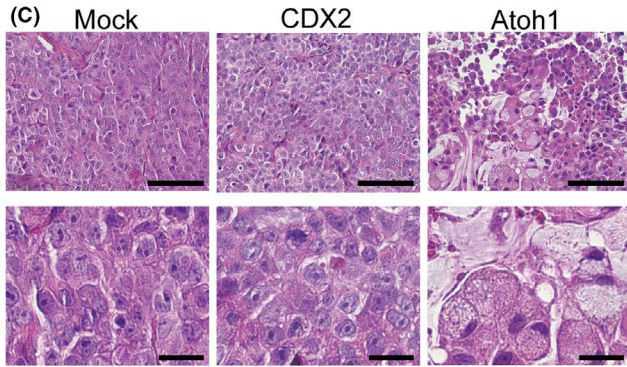


TABLE 2 Comprehensive gene expression of Atoh1-expressing tumors was evaluated by microarray analysis

PANC1 vs Atoh1	Fold change ≥ 500		PANC1/ Atoh1
	PANC1	Atoh1	
Gene name	Normalized	Normalized	Fold change
TFF3	0.020	157.4	7787.1
AGT	0.005	38.8	7231.0
CEACAM5	0.006	17.6	2948.6
CLRN3	0.005	12.9	2620.7
CEACAM6	0.007	18.3	2573.1
TTR	0.005	12.1	2262.9
REG4	0.020	37.0	1804.0
AGR2	0.083	131.0	1570.9
FMOD	0.050	75.2	1510.8
MYOC	0.008	9.5	1145.6
LGALS4	0.20	225.9	1143.0
LINC00261	0.006	6.3	1096.8
HEPACAM2	0.005	5.2	947.5
TSPAN8	0.021	16.6	809.6
FXYD3	0.037	27.6	739.9
PEG10	0.008	5.6	691.3
GPA33	0.006	4.2	688.8
PHGR1	0.020	13.6	683.8
INSM1	0.006	4.2	674.4
PRR15L	0.015	9.0	615.1
AGR3	0.005	2.4	502.1

Microarray analysis revealed genes upregulated by >500-fold change in Atoh1-expressing cells relative to wild type Panc1 cells.

Atoh1 was upregulated in the high-grade region compared with the low-grade region of IPMN in identical patients. Additionally, the Atoh1 expression was maintained in the invasive region of IPMN, suggesting that the intestinal phenotype during tumor progression in IPMN is maintained by Atoh1. Previous reports have shown that MUC2 was directly induced by CDX2 in intestinal-type IPMN,²⁶ as it has been believed that CDX2 alone could establish intestinal metaplasia and MUC2 expression in IPMN. In the intestine, various types of epithelial cells, such as goblet cells, Paneth cells, enteroendocrine cells, and enterocytes, are differentiated from intestinal epithelial stem cells based on the differentiation cascade regulated by transcription factors.¹² MUC2, which is specifically expressed in goblet cells, is regulated by not only CDX2 but also by a series of these transcription factors in the differentiation cascade. Atoh1 is one of the most important transcription factors for the differentiation toward the secretory lineage of intestinal epithelial cells, goblet cells, Paneth cells, and enteroendocrine cells. Atoh1 also participates in the intestinal metaplasia of gastric mucosa²⁷ and Barrett's esophagus,²⁸ suggesting that systematic regulation of intestinal differentiation

is involved in intestinal-type IPMN. In the present study, Atoh1 expression in intestinal-type IPMN suggested that Atoh1 induced the expression of the secretory lineage phenotypic genes of the intestine in pancreatic cells. More number of cases should, however, be analyzed to provide general information in future.

To confirm the role of Atoh1 in intestinal-type IPMN, we attempted to induce Atoh1 expression in pancreatic cells. To our knowledge, no study has reported the functional analysis of CDX2 and Atoh1 in pancreatic cells, although several reports have described the histochemical analysis of CDX2 expression in IPMN. Hence, the present study is the first to evaluate the effect of overexpression of either CDX2 or Atoh1 on the intestinal phenotype in pancreatic cells. Panc1 cell line is commonly used as PDAC, in which CDX2 and Atoh1 are not expressed. Although both CDX2 and Atoh1 were successfully expressed in Panc1 cells, only Atoh1 could induce MUC2 expression in the pancreatic cell line. In the present study, CDX2 alone could not induce Atoh1 expression. We have reported that Atoh1 expression was regulated by not only CDX2 but also by Notch signaling,¹⁷ as the balance between CDX2 and Notch signal might be not suitable for Atoh1 induction in Panc1 cells. Although we attempted to confirm whether Atoh1 can induce intestinal phenotype, including CDX2 and MUC2 expression, using the other PDAC cell lines, we observed that neither CDX2 nor Atoh1 induced the intestinal phenotype. Therefore, the functional analysis of Atoh1 and CDX2 in intestinal-type IPMN requires further experiments to elucidate the molecular mechanism of intestinal metaplasia in pancreatic cells. However, Atoh1-expressing cells exhibited the expression of CDX2 and MUC2 in pancreatic cells, suggesting that these cells in the pancreas mimic the phenotype of intestinal-type IPMN. As anticipated, Atoh1-expressing tumors generated from Atoh1-expressing Panc1 cells by xenograft transplantation demonstrated mucinous formation such as the colloid carcinoma of intestinal-type IPMN. Furthermore, microarray analysis revealed a similar expression of Atoh1-expressing tumors to that of intestinal-type IPMN, such as TFF3,²⁹ REG4,²⁰ and MUC13.²¹ We had earlier reported that HD-6, which exerts an antimicrobial activity and is expressed in Paneth cells of the human small intestine, was directly induced by Atoh1 in intestinal epithelial cells.¹⁹ We had also reported that HD-6 was ectopically expressed in mucinous colon carcinoma where Atoh1 was expressed.³⁰ In the present study, we detected the expression of HD-6 in Atoh1-expressing IPMN, indicating that Atoh1 regulates the intestinal phenotype of intestinal-type IPMN. Furthermore, HD-6 was expressed in Atoh1-expressing tumors derived from Atoh1-expressing Panc1 cells, suggesting that Atoh1-expressing tumors comprise a useful tool as a model of intestinal-type IPMN. All intestinal phenotypic genes are not automatically expressed in intestinal epithelial cells. Although CDX2 and Atoh1 are expressed in both small intestine and colon, the genes expressed in small intestine are different from that in colon. It therefore remains unknown which intestinal phenotypic genes are expressed in intestinal-type IPMN. In the present study, we could efficiently identify the intestinal phenotypic genes expressed in intestinal-type IPMN by generating a Atoh1-expressing pancreatic tumor.

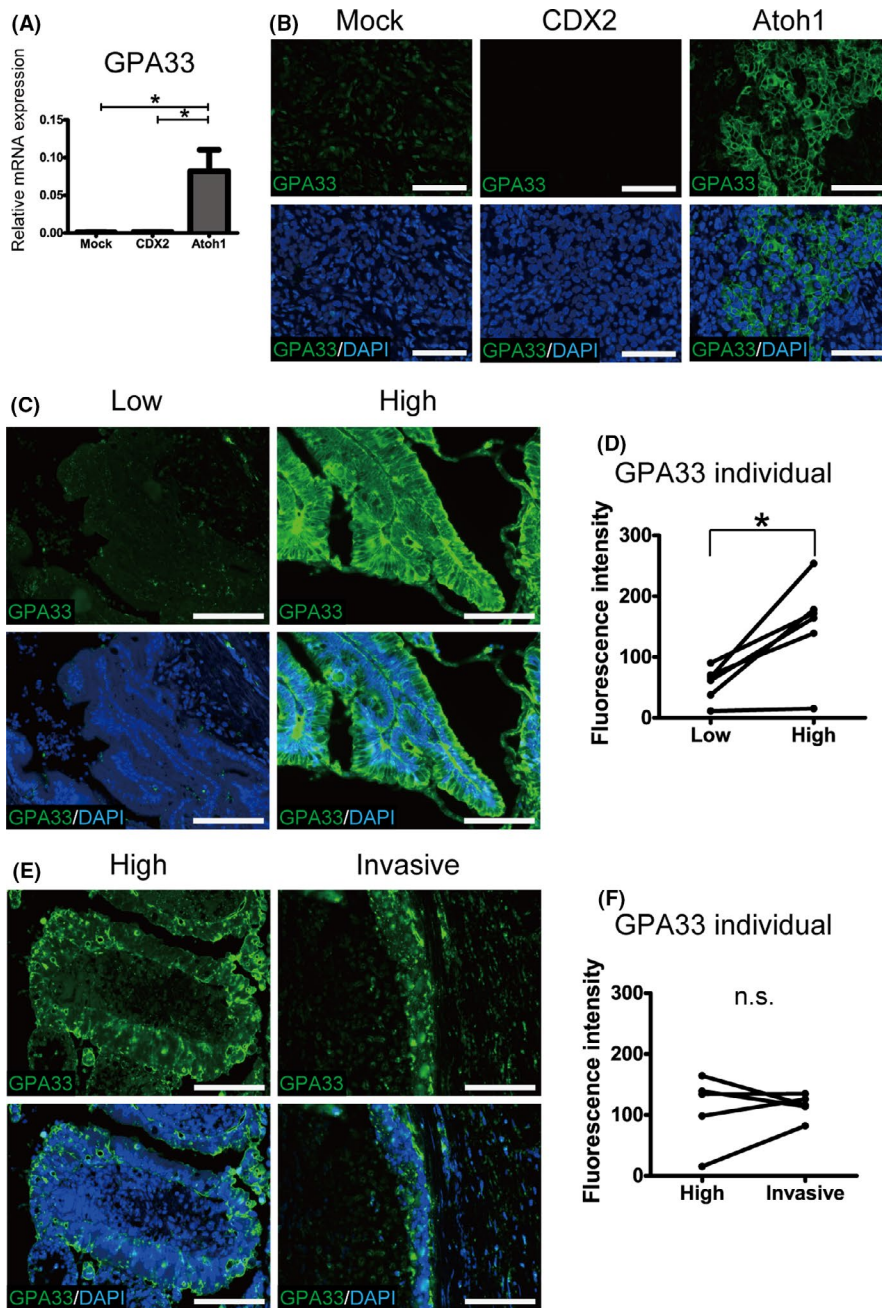


FIGURE 5 Atoh1 enhances the expression of GPA33 in IPMN. **A**, RT-PCR analysis of GPA33 in xenograft. * $P < .05$, $n = 3$. **B**, Immunofluorescence staining of GPA33 in xenograft revealed that GPA33 was induced by Atoh1-expressing tumors but not CDX2-expressing tumors. Scale bars, 100 μm . **C**, Immunofluorescence staining of GPA33 in a section of low-grade and high-grade IPMN (patient no. 7). Scale bars, 100 μm . **D**, Immunofluorescence intensity of GPA33 in a section of low-grade and high-grade IPMN was quantified. The dots of the same patient were connected by a line. An identical comparison between 6 patients with low-grade or high-grade IPMN revealed that the expression levels in high-grade IPMN were significantly higher than that in low-grade IPMN. * $P < .05$. **E**, Immunofluorescence staining of GPA33 in a section of high-grade and invasive IPMN (patient no. 9). Scale bars, 100 μm . **F**, The immunofluorescence intensity of GPA33 in a section of high-grade and invasive IPMN was quantified. The dots of the same patient were connected by a line. An identical comparison between the high-grade and invasive regions of 5 patients revealed that the expression level in invasive IPMN was equal to that in high-grade IPMN

Microarray analysis of Atoh1-expressing tumors disclosed a novel marker expressed in intestinal-type IPMN. GPA33 exhibited a broader expression in almost all intestinal epithelial cells of both small intestine and colon compared with CDX2.²² Furthermore, GPA33 was expressed in intestinal metaplasia-based cancers such as Barrett's esophageal cancer and intestinal-type gastric cancer.^{24,25} In the present study, for the first time, we discovered the expression of GPA33 in intestinal-type IPMN in parallel with induction of CDX2 and Atoh1 during tumor progression of IPMN. In particular, GPA33 was recently presumed to be a novel target for the treatment of colon cancer, based on its high expression level of 95% in primary and metastatic colon cancers.²³ A clinical trial demonstrated the selective and rapid localization of humanized monoclonal antibody for GPA33 to colorectal carcinoma without

any severe side effects to the intestine.^{31,32} Furthermore, GPA33 antigen-mediated radioimmunotherapy (RIT) demonstrated significant antitumor effects and successfully reduced radioactive toxicity to nontarget organs in the first in-human trial.^{33,34} Additionally, GPA33 antibody was expected to be useful as a delivery tool in cancer therapy. GPA33 antibody combined with exosomes involving doxorubicin have demonstrated an excellent tumor-targeting ability both in vitro and in vivo.³⁵ Using animal models, GPA33 antibody was developed in combination with CD3 antibody and resulted in tumor growth inhibition.³⁶ Altogether, the development of cancer therapy using GPA33 antibody might be useful in the therapy of GPA33-positive IPMN.^{37,38} Although GPA33 was expressed in all samples of intestinal-type IPMN in the present study, conducting further analysis using a large number

of samples is necessary to understand the frequency of GPA33-positive cancer in IPMN.

Finally, we discuss the relationship between the role of Atoh1 in IPMN and intestinal phenotype during tumor progression in IPMN. Unfortunately, we could establish only 1 pancreatic cell line with functionalized Atoh1, therefore the function of Atoh1 in pancreatic cells remains unknown. However, the results observed in Atoh1-expressing tumors in the xenograft model were sufficient to explain the phenomenon during tumor progression in intestinal-type IPMN. Atoh1 exerts different roles in tumorigenesis in different types of tumors. It serves as a tumor suppressor in Merkel cell carcinoma and sporadic colon cancer, whereas it becomes an oncogene in small-cell lung carcinoma and mucinous colon cancer.^{13,30} In the present study, Atoh1-expressing tumors exhibited significant tumor growth that displayed frequent cancer stem cells. This finding suggested that Atoh1 acts as an oncogene for tumor progression of intestinal-type IPMN. MUC13 and REG4, both of which were induced in Atoh1-expressing tumors, have also been reported as intestinal phenotypic genes that were upregulated during tumor progression of intestinal-type IPMN. In particular, MUC13 expression in IPMN has been associated with poor prognosis,²¹ suggesting that intestinalization is related to the acquisition of malignant potential during tumor progression of intestinal-type IPMN. To determine whether Atoh1 was more essential than CDX2 in acquiring the intestinal phenotype in IPMN, further analysis using numerous pancreatic cells such as organoids is needed in the future.

To our knowledge, this study is the first to evaluate Atoh1 expression in intestinal-type IPMN. Atoh1 overexpression in pancreatic cells indicated a way to mimic tumor progression of intestinal-type IPMN. GPA33 identified from Atoh1-expressing tumors was found for the first time to be expressed in intestinal-type IPMN. Intestinal phenotypic genes might be potential targets in cancer therapy for intestinal-type IPMN. Further functional analysis of intestinal differentiation-regulating genes, such as CDX2 and Atoh1, might be useful to understand the molecular mechanisms underlying tumor progression of IPMN and the accumulation of gene mutations.

ACKNOWLEDGMENTS

This work was supported by scientific Research from the Japanese Ministry of Education, Culture, Sports, Science and Technology (KAKENHI grant numbers 17H06654, 17K15930, 17K19513, 17K159301, 18H02791); the Japan Foundation for Applied Enzymology; a Health and Labor Sciences Research Grant from the Japanese Ministry of Health, Labor and Welfare (grant number 14526073); The Practical Research for Innovative Cancer Control, Rare/Intractable Diseases from Japan Agency for Medical Research and Development (AMED) (grant numbers 15Ack0106017h0002, 16ck0106017h0003); and a Research Grant from the Princess Takamatsu Cancer Research Fund. The authors would like to thank Enago (www.enago.jp) for English language review.

CONFLICT OF INTEREST

The authors have no conflicts of interest to disclose.

ORCID

Ryuichi Okamoto  <https://orcid.org/0000-0002-7047-571X>

Kiichiro Tsuchiya  <https://orcid.org/0000-0002-1977-8707>

REFERENCES

- Machado NO, Al Qadhi H, Al WK. Intraductal Papillary Mucinous Neoplasm of Pancreas. *N Am J Med Sci*. 2015;7:160-175.
- Tan MC, Basturk O, Brannon AR, et al. GNAS and KRAS Mutations Define Separate Progression Pathways in Intraductal Papillary Mucinous Neoplasm-Associated Carcinoma. *J Am Coll Surg*. 2015;220:845-854.
- Lee JH, Kim Y, Choi JW, Kim YS. KRAS, GNAS, and RNF43 mutations in intraductal papillary mucinous neoplasm of the pancreas: a meta-analysis. *Springerplus*. 2016;5:1172.
- Farrell JJ. Intraductal papillary mucinous neoplasm to pancreas ductal adenocarcinoma sequence and pancreas cancer screening. *Endosc Ultrasound*. 2018;7:314-318.
- Omori Y, Ono Y, Tanino M, et al. Pathways of progression from Intraductal papillary mucinous neoplasm to pancreatic ductal adenocarcinoma based on molecular features. *Gastroenterology*. 2019;156:647-661.
- Furukawa T, Klöppel G, Volkan Adsay N, et al. Classification of types of intraductal papillary-mucinous neoplasm of the pancreas: a consensus study. *Virchows Arch*. 2005;447:794-799.
- Furukawa T, Hatori T, Fujita I, et al. Prognostic relevance of morphological types of intraductal papillary mucinous neoplasms of the pancreas. *Gut*. 2011;60:509-516.
- Taki K, Ohmuraya M, Tanji E, et al. GNAS(R201H) and Kras(G12D) cooperate to promote murine pancreatic tumorigenesis recapitulating human intraductal papillary mucinous neoplasm. *Oncogene*. 2016;35:2407-2412.
- Adsay NV, Merati K, Basturk O, et al. Pathologically and biologically distinct types of epithelium in intraductal papillary mucinous neoplasms: delineation of an "intestinal" pathway of carcinogenesis in the pancreas. *Am J Surg Pathol*. 2004;28:839-848.
- Omori Y, Ono Y, Kobayashi T, et al. How does intestinal-type intraductal papillary mucinous neoplasm emerge? CDX2 plays a critical role in the process of intestinal differentiation and progression. *Virchows Arch*. 2020;477:21-31.
- Yang Q, Bermingham NA, Finegold MJ, Zoghbi HY. Requirement of Math1 for secretory cell lineage commitment in the mouse intestine. *Science*. 2001;294:2155-2158.
- Nakamura T, Tsuchiya K, Watanabe M. Crosstalk between Wnt and Notch signaling in intestinal epithelial cell fate decision. *J Gastroenterol*. 2007;42:705-710.
- Fu Y, Yuan SS, Zhang LJ, Ji ZL, Quan XJ. Atonal bHLH transcription factor 1 is an important factor for maintaining the balance of cell proliferation and differentiation in tumorigenesis. *Oncol Lett*. 2020;20:2595-2605.
- Nagtegaal ID, Odze RD, Klimstra D, et al. The 2019 WHO classification of tumours of the digestive system. *Histopathology*. 2020;76:182-188.
- Kano Y, Tsuchiya K, Zheng X, et al. The acquisition of malignant potential in colon cancer is regulated by the stabilization of Atonal homolog 1 protein. *Biochem Biophys Res Commun*. 2013;432:175-181.
- Tsuchiya K, Nakamura T, Okamoto R, Kanai T, Watanabe M. Reciprocal targeting of Hath1 and beta-catenin by wnt glycogen synthase kinase 3 beta in human colon cancer. *Gastroenterology*. 2007;132:208-220.
- Zheng X, Tsuchiya K, Okamoto R, et al. Suppression of hath1 gene expression directly regulated by hes1 via notch signaling is associated with goblet cell depletion in ulcerative colitis. *Inflamm Bowel Dis*. 2011;17:2251-2260.
- Kobayashi M, Fujinaga Y, Ota H. Reappraisal of the Immunophenotype of Pancreatic Intraductal Papillary Mucinous

- Neoplasms (IPMNs)-Gastric Pyloric and Small Intestinal Immunophenotype Expression in Gastric and Intestinal Type IPMNs. *Acta Histochem Cytochem*. 2014;47:45-57.
19. Hayashi R, Tsuchiya K, Fukushima K, et al. Reduced Human alpha-defensin 6 in Noninflamed Jejunal Tissue of Patients with Crohn's Disease. *Inflamm Bowel Dis*. 2016;22:1119-1128.
 20. Nakata K, Nagai E, Ohuchida K, et al. REG4 is associated with carcinogenesis in the 'intestinal' pathway of intraductal papillary mucinous neoplasms. *Mod Pathol*. 2009;22:460-468.
 21. Mito K, Saito M, Morita K, et al. Clinicopathological and prognostic significance of MUC13 and AGR2 expression in intraductal papillary mucinous neoplasms of the pancreas. *Pancreatol*. 2018;18:407-412.
 22. Johnstone CN, White SJ, Tebbutt NC, et al. Analysis of the regulation of the A33 antigen gene reveals intestine-specific mechanisms of gene expression. *J Biol Chem*. 2002;277:34531-34539.
 23. Wong N, Adamczyk LA, Evans S, Cullen J, Oniscu A, Oien KA. A33 shows similar sensitivity to but is more specific than CDX2 as an immunomarker of colorectal carcinoma. *Histopathology*. 2017;71:34-41.
 24. Lopes N, Bergsland C, Bruun J, et al. A panel of intestinal differentiation markers (CDX2, GPA33, and LI-cadherin) identifies gastric cancer patients with favourable prognosis. *Gastric Cancer*. 2020;23:811-823.
 25. Wong NA, Warren BF, Piris J, Maynard N, Marshall R, Bodmer WF. EpCAM and gpA33 are markers of Barrett's metaplasia. *J Clin Pathol*. 2006;59:260-263.
 26. Yamamoto H, Bai YQ, Yuasa Y. Homeodomain protein CDX2 regulates goblet-specific MUC2 gene expression. *Biochem Biophys Res Commun*. 2003;300:813-818.
 27. Zhang X, Yang Y, Zhu R, et al. H. pylori induces the expression of Hath1 in gastric epithelial cells via interleukin-8/STAT3 phosphorylation while suppressing Hes1. *J Cell Biochem*. 2012;113:3740-3751.
 28. Kong J, Crissey MA, Sepulveda AR, Lynch JP. Math1/Atoh1 contributes to intestinalization of esophageal keratinocytes by inducing the expression of Muc2 and Keratin-20. *Dig Dis Sci*. 2012;57:845-857.
 29. Terris B, Blaveri E, Crnogorac-Jurcevic T, et al. Characterization of gene expression profiles in intraductal papillary-mucinous tumors of the pancreas. *Am J Pathol*. 2002;160:1745-1754.
 30. Fukushima K, Tsuchiya K, Kano Y, et al. Atonal homolog 1 protein stabilized by tumor necrosis factor alpha induces high malignant potential in colon cancer cell line. *Cancer Sci*. 2015;106:1000-1007.
 31. Scott AM, Lee FT, Jones R, et al. A phase I trial of humanized monoclonal antibody A33 in patients with colorectal carcinoma: biodistribution, pharmacokinetics, and quantitative tumor uptake. *Clin Cancer Res*. 2005;11:4810-4817.
 32. Welt S, Ritter G, Williams C Jr, et al. Preliminary report of a phase I study of combination chemotherapy and humanized A33 antibody immunotherapy in patients with advanced colorectal cancer. *Clin Cancer Res*. 2003;9:1347-1353.
 33. Chong G, Lee FT, Hopkins W, et al. Phase I trial of 131I-huA33 in patients with advanced colorectal carcinoma. *Clin Cancer Res*. 2005;11:4818-4826.
 34. Zanzonico P, Carrasquillo JA, Pandit-Taskar N, et al. PET-based compartmental modeling of (124I)-A33 antibody: quantitative characterization of patient-specific tumor targeting in colorectal cancer. *Eur J Nucl Med Mol Imaging*. 2015;42:1700-1706.
 35. Li Y, Gao Y, Gong C, et al. A33 antibody-functionalized exosomes for targeted delivery of doxorubicin against colorectal cancer. *Nanomedicine*. 2018;14:1973-1985.
 36. Moore PA, Shah K, Yang Y, et al. Development of MGD007, a gpA33 x CD3-Bispecific DART Protein for T-Cell Immunotherapy of Metastatic Colorectal Cancer. *Mol Cancer Ther*. 2018;17:1761-1772.
 37. Murer P, Plüss L, Neri D. A novel human monoclonal antibody specific to the A33 glycoprotein recognizes colorectal cancer and inhibits metastasis. *MAbs*. 2020;12:1714371.
 38. Wei D, Tao Z, Shi Q, et al. Selective Photokilling of Colorectal Tumors by Near-Infrared Photoimmunotherapy with a GPA33-Targeted Single-Chain Antibody Variable Fragment Conjugate. *Mol Pharm*. 2020;17:2508-2517.

SUPPORTING INFORMATION

Additional supporting information may be found online in the Supporting Information section.

How to cite this article: Katsukura N, Watanabe S, Shirasaki T, et al. Intestinal phenotype is maintained by Atoh1 in the cancer region of intraductal papillary mucinous neoplasm. *Cancer Sci*. 2021;112:932-944. <https://doi.org/10.1111/cas.14755>